Sensor Optimization for Fault Diagnosis in Multi-Fixture Assembly Systems With Distributed Sensing

A. Khan

D. Ceglarek[1]
e-mail: darek@engin.umich.edu

S. M. Wu Manufacturing Research Center,
The University of Michigan,
Ann Arbor, MI 48109

Sensing for the system-wide diagnosis of dimensional faults in multi-fixture sheet metal assembly presents significant issues of complexity due to the number of levels of assembly and the number of possible faults at each level. The traditional allocation of sensing at a single measurement station is no longer sufficient to guarantee adequate fault diagnostic information for the increased parts and levels of a complex assembly system architecture. This creates a need for an efficient distribution of limited sensing resources to multiple measurement locations in assembly. The proposed methodology achieves adequate diagnostic performance by configuring sensing to provide an optimally distinctive signature for each fault in assembly. A multi-level, two-step, hierarchical optimization procedure using problem decomposition, based on assembly structure data derived directly from CAD files, is used to obtain such a novel, distributed sensor configuration. Diagnosability performance is quantified in the form of a defined index, which serves the dual purpose of guiding the optimization and establishing the diagnostic worth of any candidate sensor distribution. Examples, using a multi-fixture layout, are presented to illustrate the methodology. [S1087-1357(00)70801-X]

1 Introduction

The dual requirements of system-level fault diagnosis are that the presence of malfunctioning module(s) be identified, and the fault root cause isolated to the responsible element(s) of the system. The guarantee of optimal diagnosis for sheet metal assembly is a pragmatic satisfaction of both these requirements: by best identifying the manifestation of misbehavior, and by providing the best localization and isolation of dimensional failure. For complex systems, one systematic approach to laying the foundation for diagnosis is to synthesize the modes of operation (or failure) a-priori; by working from elemental functionality (loss of functionality) towards module behavior (misbehavior). Sensor position and distribution may then be tailored to best capture such misbehavior.

In the context of system complexity, the complement of two hundred fixtures, each with multiple part locators, used in the assembly of the typical automobile Body-in-White (BIW) serves as a case in point. Conventional fault diagnosis in BIW assembly relies on sensing at a single location [1], typically at the end of an assembly line. Compared to this end-of-line sensing approach, distributed sensing, performing measurements at multiple different points in assembly, presents clear advantages. These include a natural decomposition of the fault localization and isolation tasks (limiting it to assembly stations upstream of the sensing-measurement station). Figure 1 captures the distinction between the two approaches.

However, as each fixture in the distributed sensing paradigm now becomes a prospective measurement station, there is a significant increase in the complexity of implementation. This stems from the need to formalize, for each level in an assembly hierarchy, an efficient allocation scheme for the available sensor set, the constraints imposed by practical assembly considerations, an estimate of redundancy in fault coverage, etc. Allocation involves first, the choice of measurement stations best suited for sensor coverage along with a choice of a certain number of measurement points for each station, and second, the specific location of each of the sensors at the station. The efficient handling of such details is crucial to the success of a comprehensive distributed sensing scheme. In this paper, we propose the means to incorporate such information directly in the problem formulation, and optimize over a generated set of feasible candidate (measurement station) configurations.

1.1 Fixture Failure Diagnosis. In an assembly system, defects in the final product or in subassemblies are ultimately manifestations of failure of element(s) of the system tooling. The first step in diagnosis is thus usually the creation of a listing of categories of failure, or failure modes. This section describes the failure categorization utilized for sensor optimization implementation. The traditional diagnosis method involves first creating a behavior set for the system, then proceeding to catalog all possible failure types along with the related root-cause of failure [2,3]. However, an enumerative approach quickly becomes overwhelming, especially when applied to a complex system [4].

A way out of this difficulty is to exploit domain structure in such systems, whenever such a structure is discernible. Thus, to directly formulate the failure modes for sheet metal assembly [5], a CAD-based design description of assembly system structure is used. This approach reduces dependance on domain experiential knowledge (ad hoc rules) and domain historical knowledge (probabilistic rule-bases) as primary sources of behavioral information. Another critical advantage of this approach is simplification. Given that a disadvantage of the growth in system complexity is the proportional increase in the difficulty in identifying all failure modes to be diagnosed [6], any approach that ''automatically'' converts structural information to formulate fault information holds additional promise. Also, structure descriptions available in CAD databases are well organized and functionally complete. A catalog of misbehavior from such a source inherits these traits—of being systematically constructed, modular, and descriptively complete.

In BIW assembly, fault behavior or defects are described di-

[1]Corresponding author.

Contributed by the Manufacturing Engineering Division for publication in the JOURNAL OF MANUFACTURING SCIENCE AND ENGINEERING. Manuscript received Dec. 1997; revised July 1998. Associate Technical Editor: M. Elbestawi.

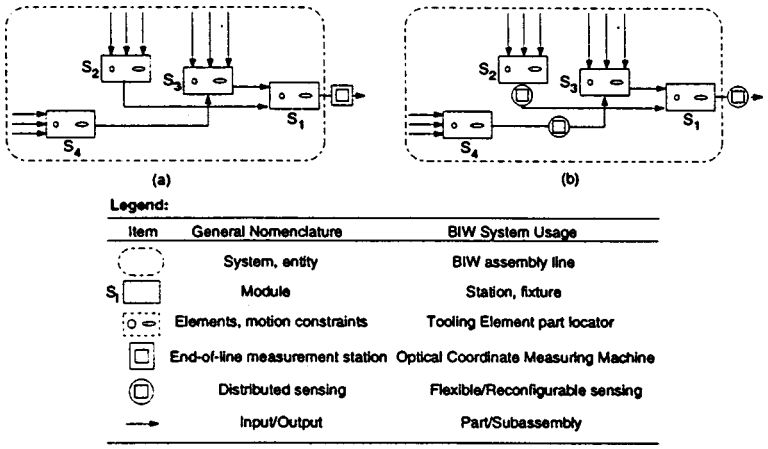

Fig. 1 Sensing approaches: (*a*) end-of-line sensing, (*b*) distributed sensing

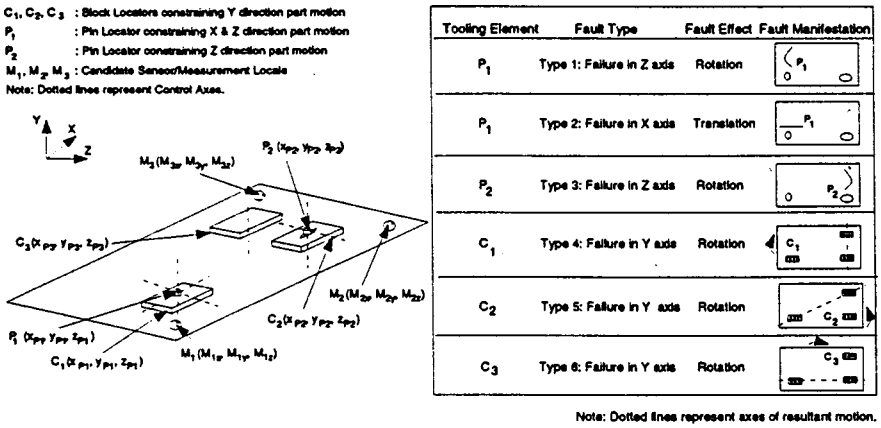

Fig. 2 Generic 3-2-1 fixture layout and corresponding failure mode fault manifestations

mensionally. Dimensional inconsistency among parts or subassemblies are typically measured with Optical Coordinate Measuring Machine (OCMM) laser sensors and reported as dimensional variation. The statistical extent of variation is a measure of the magnitude of the fault. Exploitable information on fixture structure, available in CAD databases, consists of the dimensional location of all constraint-providing Tooling Element (TE) part or subassembly locators. The shapes and position of TEs are designed to fulfill the requirements of repeatable part location and constraint during assembly. A categorization of failure is achieved by associating a loss of constraint of each of these TEs along a specific direction, with the resultant part motion during failure. Figure 2 illustrates this for a conventional 3-2-1 fixture configuration. The fault types enumerated for the given TE set of block locators C_i, $i=1,\ldots,3$, and pins P_j, $j=1,2$, are exhaustive for the configuration [5]. Details of the sensor allocation methodology for single fixture fault diagnosability enhancement, based on such a fault categorization, are provided in Khan et al. [7].

1.2 Assembly System Hierarchy. Domain structure gleaned from a CAD database (TE locator coordinate data) is essentially ''knowledge in isolation,'' comprising detailed information on system components (fixtures, parts/subassemblies). To incorporate a system viewpoint, isolated information can be integrated to establish dependencies and reflect sequence, using a graphical metaphor. This positions fixture-specific information in the context of the overall assembly hierarchy. Such a representation used to capture sequence information for optimization, is discussed here.

A directed graph State-Transition $\langle \mathbf{X}\ \mathbf{T} \rangle$ representation of the assembly process provides the framework for reasoning on the knowledge and for evaluating alternatives. This utility provides the basis for the optimization approach. Nodes in the representation correspond to states of assembly $\mathbf{X}$, with transitions $\mathbf{T}$ reflecting assembly operations which cause a change of state. For N assembly states, there is a set of N partitions Θ_l, $l=1,\ldots,N$, each comprising individual elements θ_i. The index i tracks an individual element at level l. For the widget assembly of Fig. 3(*a*), the initial state of the $\langle \mathbf{X}\ \mathbf{T} \rangle$ of Fig. 3(*b*) is represented by partition $\{\{A\}\{B\}\{C\}\{D\}\}$ at level $l=4$, with individual elements (representing parts) $\{A\}$, $\{B\}$, $\{C\}$, and $\{D\}$; and the final state by the partition $\{\{ABCD\}\}$ at level $l=1$, with a single element (representing the end product of assembly) $\{ABCD\}$. The representation's isomorphic characteristic ensures a consistency of sequence and interconnection with the physical assembly structure. The sensor layout optimization algorithm works by allocating sensing resources to this structure, reflecting a sensor distribution to fixtures in an assembly. Simultaneously, it evaluates overall diagnostic performance, reflecting a sensor layout's fault discrimination capability. This paradigm thus provides a transparent analytical capability through mapping even intermediate steps in the optimi-

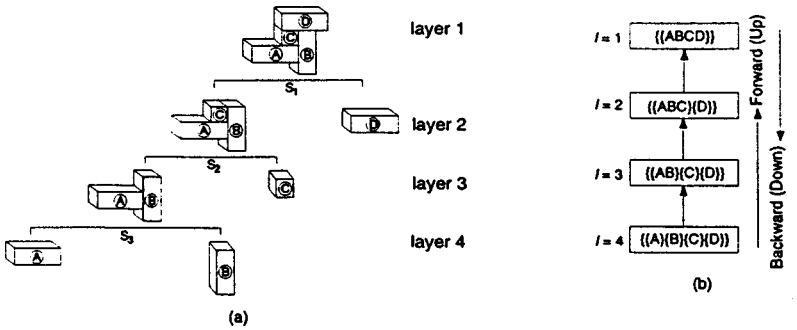

Fig. 3 Assembly representation for optimization for (*a*) the example four-part widget assembly (S_1, S_2, S_3 represent assembly stations), (*b*) state-transition representation (for each level l,$\{\{\Theta\}\}$ is a partition representing assembly state, with element $\{\theta_l\}$ representing a subassembly or part)

zation to the assembly structure, allowing for an intuitively meaningful interpretation of the sensor layout. The assembly process representation shares the characteristics of and is modeled after De Fazio and Whitney [8], and Homem de Mello and Sanderson [9]. Details of the structure formulation, as used for multi-fixture end-of-line sensor allocation, are provided in Khan et al. [10].

The following section presents distributed sensing as a logical extension of the schemes developed for single fixture and end-of-line sensing allocation discussed above. The criteria for implementation feasibility in practice are also discussed. This is followed by a description of the optimization approach to distributed sensing implementation. Finally, applications using a multi-fixture assembly layout are presented to illustrate the methodology.

2 Distributed Sensing

Both the extent to which a diagnosis explains a fault's symptom set (fault isolation), and the extent of the faithfulness with which a symptom set manifests any fault behavior (fault identification), may be postulated as functions of sensing performance. More fundamentally, sensing performance is intrinsically a function of the effectiveness of the sensor hardware utilized. Given a specific choice of sensor hardware, and assuming uniform sensing ability of all sensors in the given set however, leaves only the allocation of sensors as the variable influencing sensing capability. The allocation problem requires a decision on both measurement station locations along with the number of sensors at each, and a decision on the exact positioning of the sensors at the stations.

2.1 Sensor Allocation Schemes. The specific requirements of the problem, available sensing resources, and problem constraints, determine the choice of the allocation scheme—local single fixture, end-of-line, or distributed—used to provide optimal sensing.

Local single fixture sensing involves sensing at the immediate location of the failure. A condition of local sensing is that the deployed sensor set aims only to localize faults originating within the fixture under consideration. This excludes faults which occur as a repercussion of failure at a separate fixture. Such failures, because of their position in assembly, can exert an influence on the fixture under consideration. Being focused exclusively on the one fixture, an optimal single fixture sensor locale diagnoses with a high degree of precision, the location and mode of failure of faults within that fixture.

End-of-line sensing involves monitoring fault manifestations at a single location, not necessarily immediate to the failure, to diagnose all failure types in a system. Such sensing is typically performed at a measurement station at the end of an assembly line (Fig. 1(*a*)). The problem is one of achieving localized fault identification based on a global manifestation of the evidence in the end-of-line product. This problem is characterized by significant complexity due to the multiple faults which need to be diagnosed from measurements at this single location. Whenever possible, explicit independencies in the problem may be exploited to obtain order of magnitude reductions in complexity. In addition, independencies found for each of several decomposed subproblems are used to achieve optimality of sensor distribution at the subcomponent level. Such optimalities may then be coordinated at a higher level to obtain an overall optimality. The Hierarchical Decision Making approach [10] used to implement this, provides that each decision affect the circumstances under which the next decision is made. This ensures the overall integration of subcomponent optimalities. Such an overall optimal sensor locale for the end-of-line measurement station provides an overall optimal diagnosability.

In complex systems, the traditional approach is to provide sensors at a single measurement station, charged with the task of diagnosing faults in multiple part assemblies, at multiple levels of assembly. As the number of parts and levels increase, the Maximum Effective Depth criteria [10], reveals shortcomings in the ability of this single station to distinguish between fault manifestations for diagnosis. *Distributed sensing* aims to enhance the information content available from the sensor set by reallocating and distributing sensors at multiple measurement stations throughout the assembly. As the presence of a fault is best detected at its inception, a distributed sensing scheme offers an inherently higher probability of recording faults immediately following their occurrence. Also, by distributing the sensing assignment to a combination of local, intermediate, and end-of-line locations, the mechanism records a more comprehensive and distinctive signature-set description for faults.

To foster confidence in the resultant diagnosis, a critical need is to enhance the sensing scheme's discrimination performance. This provides for quick fault detection and reduces the number of alternative fault scenarios which need to be evaluated for diagnosis. The optimization objective is to create a locale which generates a fault signature unequivocally distinct in manifestation from any other. Thus, in comparison to end-of-line sensing, an optimal distributed sensing scheme achieves improvements at two levels—by enhancing the ability of the sensors to serve as fault identification indicators, and by enhancing their distinctiveness as fault isolation indicators.

2.2 Sensing Criteria and Considerations: BIW Assembly. For the BIW case, information deemed to be descriptively complete for the purpose of optimization includes:

1 a description of structure (the fixtures involved),
2 a description of inputs (number and geometry of the parts involved), and
3 a description of outputs (sensor readings of the measured product or subassemblies).

The objective is to provide fault isolation with algorithmic certainty by utilizing this complete knowledge domain.

Constraints on sensor position are typically part of the problem description. These usually take the form of areas of the fixture blacked-out (or unavailable) for use in sensor allocation. In addition to unavailable areas, other constraints need to be incorporated to reflect restrictions on the available number in the sensor set, those allocatable to specific stations only, or those available only for the measurement of certain subassemblies.

In addition to the book-keeping complexity involved in suitably applying such constraints, a distributed sensing scheme also has to accommodate and consider each of the multiple stations as viable alternatives for sensor location. Any proposed final locale specification will need to have satisfactorily addressed:

1 which measurement stations or fixture combinations are best suited for sensor coverage,
2 the number of measurement points required at each measurement station, and
3 sensor redundancy to provide (a) a performance enhancement to an accompanying sensor to help localize a single fault, or (b) working in tandem with a remotely located sensor to diagnose a class of faults, or both.

Distributed sensing thus trades off additional complexity to formulate a constraint-satisfying sensing solution, with the opportunity to significantly enhance fault discrimination and localization.

3 Sensor Allocation Optimization

The optimization approaches which have been developed (cited in the following sections), address successive enhancements in system complexity: from local sensing at a single fixture, to end-of-line sensing for multiple fixtures, and finally to the focus of this paper—distributed sensing for multiple fixtures.

3.1 Local Single Fixture Sensing Optimization. For a 3-2-1 single fixture configuration with local sensing (as in Fig. 2), the set of all possible fault descriptions [5] may be captured in the form of a signature matrix of six diagnostic vectors, $\mathbf{d(i)}, i = 1, \ldots, 6$. These correspond to part constraint failures along the six possible degrees of freedom. The performance of an optimal sensor locale at localizing members of this fault set for diagnosis may be determined using the formulation for the optimal Diagnosability index [7] performance measure, J^*_{opt}:

$$J^*_{\text{opt}} = \forall_{i \neq j} \max \left[\min \sum_{i=1,\ldots,6} \sum_{j=1,\ldots,6} W_{ij} \|\mathbf{d(i)} - \mathbf{d(j)}\| \right]$$
$$\text{s.t. } G(x,y,z) \leqslant 0 \tag{1}$$

The objective of the optimization is a maximal spread of the fault vectors in fault space. Weights W_{ij} may be constructed so as to specify the relative importance of diagnosis of specific fault types, and constraints $G(x,y,z)$ to capture constraints on sensor location in (x,y,z) part/fixture coordinates as dictated by practical considerations. The optimization of Eq. (1) results in a sensor set in which the sensor positions, constituting an optimal sensor locale, provide the best possible fault discrimination for the configuration.

3.2 End-of-line Sensing Optimization. Optimization for multi-fixture end-of-line sensing involves an evaluation of the J_{opt} formulation for all fixtures in the assembly line under consideration. This process involves (1) decomposing the assembly system into hierarchical levels in the $\langle \mathbf{X}\ \mathbf{T} \rangle$ representation Fig. 3(*b*); (2) sequential optimization level-to-level; and (3) the coordination of such subproblem optimalities using Hierarchical Decision Making, to achieve overall optimality [10]. As indicated in Fig. 3(*b*), such hierarchical optimization can proceed in two directions:

1 Forward Chaining: Forward (up) from the leaf nodes (at level 4)—the component part level, or
2 Backward Chaining: Backward (down) from the root node (at level 1)—the product level.

In the course of the optimization, information is transmitted from level to level in the form of optimal sensor locale state variables. Candidate sensor locales, evaluated for optimality at each level, are design variables with an associated sensor number design parameter. At each level, for each candidate sensor locale configuration, a transition function, $\|\mathbf{d(i)} - \mathbf{d(j)}\|$, is evaluated for the set of all pairs of diagnostic vectors. Sensor number constraints are also imposed at each level, to build up the optimal measurement station configuration with the given sensor set. The estimate of diagnostic performance of a candidate end-of-line locale is the magnitude of its Coverage Effectiveness Index, C (C_{up} and C_{dn} corresponding to Forward and Backward Chaining Approaches):

$$C = \frac{\sum_{\xi[U(gV)]} \left[\frac{J_{\text{opt}}}{J^*_{\text{opt}}} \right]}{\text{card}(\xi[U(\Theta)])} \tag{2}$$

$\xi[U(\Theta)]$ is an enumeration of all unique elements in the set of all partitions, $U[(\Theta)]$, in the hierarchy, where each partition describes an assembly state $\mathbf{X}$ (see Fig. 3(*b*)), such that $\xi[U(\Theta)] \subseteq \mathbf{X}$ and $\theta_i \neq \theta_j \forall \{\theta_i, \theta_j\} \in \xi[U(\Theta)]$, and where card $(\xi[U(\Theta)])$ is the cardinality of the set $\xi[U(\Theta)]$ of all parts or subassemblies in the assembly sequence. The local sensing optima, J^*_{opt} [Eq. (1)], corresponds to a sensor locale which provides the best possible diagnostic performance for each of the elements in $\xi[U(\Theta)]$ at a given level, without restriction on sensor locations. The optima J_{opt} reflects performance achieved by the mapping, as state variables, of an optimal locale to complement performance due to other sensors allocated at a successive level of the hierarchy. Details and the specific formulation of C_{up} and C_{dn} indices for optimization are provided in Khan et al. [10]. For a given assembly sequence, estimates of optimality achieved through each of the two (Forward and Backward Chaining) approaches are compared, and the layout corresponding to the better diagnostic performance chosen.

3.3 Distributed Sensing Optimization. Distributed sensing optimization takes place in two steps:

1 The first step of optimization determines the *number* of the available sensor resources allocated to each of the parts in assembly (incorporating the points 1 and 2 made in Section 2.2).
2 The second step of optimization then utilizes this allocation to establish the specific *location* of each sensor at an assembly station (fixture).

In the formulation for distributed sensing the constraint on the total number of available sensors as exercised in end-of-line sensing continues to be applicable. Instead of being confined to the end-of-line measurement station, however, this constrained sensor set is available for distribution throughout the hierarchy. The Hierarchical Decision Making scheme utilized in end-of-line optimization is also applicable here. The global optimal evolves from a traversal of the $\langle \mathbf{X}\ \mathbf{T} \rangle$ Representation, creating a series of optimals for each of the partitions Θ_i (levels in Fig. 3(*b*)). Developed bottom-up or top-down approaches are employed in the traversal for both the first and second steps of optimization, in a manner which parallels such a strategy for diagnosis [11]. The strategy reflects sequence during hierarchical optimization.

1 The bottom-up approach optimizes on sensor number and location at the level of the component parts first—proceeding upward in the hierarchy from the leaf nodes.
2 The top-down approach optimizes on sensor number and location at the level of the end product first—proceeding downwards in the hierarchy from the root node.

However, unlike a similar choice of order of traversal available in end-of-line sensing (forward and backward chaining), state variables are not consolidated from level to level to obtain one final, single optimal for the top (measurement station) level [10]. The optimal computed for each level is instead associated with specifying an allocation of sensors at that level.

The practical connotation of a choice of the bottom-up approach, or the top-down approach, is captured in the performance index J_{b-u} (bottom-up) or J_{i-d} (top-down), evaluated in the first step of each approach. Each reflects the specific sensing need being addressed by the choice of approach. This distinction is reflected in the optimization index definition in the First Step in each of the two approaches, as follows.

Bottom-Up Approach

1 *First Step*: This step provides the means for deciding on a sensor number allocation among the various parts of assembly. The index J_{b-u}, used to evaluated sensing performance at each stage of optimization, reflects the need to diagnose faults as soon as they occur—at the earliest stage of assembly. The focus is on immediate detection of a manifestation of the fault before its propagation in assembly. Also inherent in J_{b-u} is the assumption that sensing effort at one level, aimed at diagnosing one fault, need not be duplicated.

2 *Second Step*: This step provides the means to determine the exact coordinate location of each of the allocated sensor measurement points at the fixture or station. It involves determining the best sensor location at each part/fixture, working with the sensor number assigned to that part from the previous step. This process proceeds through the application of the equivalent of a single fixture sensing optimization approach (Section 3.1). For each fixture/measurement station with allocated sensors, the overall sensor locale is obtained as the composite mapping of such constrained single fixture optimizations for all parts assigned to that fixture/station.

Top-Down Approach

1 *First Step*: As in the bottom-up approach, this step determines the sensor number allocation to each part in the assembly. However, unlike J_{b-u}, J_{i-d} usage reflects the characterization that faults at a subassembly level may have diminished relevance to the overall end-product fault manifestation. This occurs because of the use in some assembly designs of slip-planes in the higher levels of the assembly process (in the screw-body assembly philosophy such planes are used in the final levels of assembly to absorb faults, e.g. Ceglarek and Shi [12]). Faults at the subassembly level are then subsumed, as the overall assembly absorbs the fault and is either not faulty, or manifests it as a composite fault, through a distinct signature at the end product level, or a different higher level. J_{i-d} also provides a locale which revisits fault manifestations due to failures at previous levels. Such an optimal locale guarantees overall efficiency; but with inferior discrimination performance for the revisited fault manifestations at a particular level, when compared to the corresponding J_{b-u} performance for that level.

2 *Second Step*: As in the bottom-up approach, this step specifies coordinate locations for measurement points on fixture/stations. However, the top-down approach second step involves a two-part optimization:

(a) The first part is an ''Inherent-to-Station allocation'' optimization, where a subset of the sensors allocated in the first step to the part under consideration are assigned based on the immediate local optimization needs of the fixture/station assemblies involved, as in single fixture optimization (Section 3.1).
(b) The second part is a ''Compensatory station allocation'' optimization, where the potential improvement in diagnosability due to an assignment of sensors to other locations within the hierarchy is evaluated. This is so that they may, working in tandem with the inherent sensor assignment component, capture a similar class fault manifestation at other levels in the hierarchy. Once again, this is reflective of the objective of the top-down approach, to provide supplementary fault coverage in addition to local sensing; albeit at a loss of efficiency in the local sensing component.

Thus, real-life criteria (screw-body vs. non screw-body; failure-prone vs. failure-free) may be used to dictate the approach chosen—top-down or bottom-up. At the level of the suboptimization at each step, in both bottom-up and top-down approaches, the forward and backward chaining optimization procedures originally proposed in the context of end-of-line sensing are utilized. For this we reference Khan et al. [10] to avoid repetition of implementation details. Whenever possible, optimization is initiated with an informed ''best-guess'' candidate local. Implementation is through function calls to the Matlab toolbox [13] implementing a sequential quadratic programming method. The detailed optimization procedure for both bottom-up and top-down approaches is provided in the following section, followed by an example implementation in an assembly hierarchy.

3.3.1 Optimization: Bottom-Up Approach. For purposes of generality, coverage of the set of enumerated fault conditions in the standard 3-2-1 fixture configuration is assumed to be provided by a P sensor number distribution for each part. The Maximum Effective Depth criteria, as proposed in Khan et al. [10], is used to obtain an appropriate P. This criteria was developed to help establish the specific depth, in terms of levels of assembly, which can be effectively covered (while providing adequate diagnosability performance) with a certain number of sensors from the total sensor set. The assumption of the worst case complexity is made, with the TEs locating each of the parts at the fixture being independent. The implication here is that no TE is shared between parts. The First Step and Second Step optimization procedures (Fig. 4(*a*)) involve iterating through the described step sequence, as the optimization traverses the $\langle \mathbf{X}\ \mathbf{T} \rangle$ hierarchy from the bottom up. (The steps described here are illustrated with an example in Section 4.1.1).

First Step: Number Optimization

1 For each elemental part in the hierarchy, $\theta_i, \theta_i \in \Theta_N$, local, single fixture optimization is performed to obtain individual J^*_{opt} estimates [Eq. (1)].

2 For each station in the hierarchy, forward chaining optimization is used to derive a J_{opt} for each of the $P,(P-1), \ldots,1$ sensor configurations. In the forward chaining approach, optimization is initiated at the component part level. Subsequent optimization is carried out while proceeding upwards in the hierarchy (as in Fig. 3(*b*)) using sensor locale combinations of input assembly states $\{\theta_u, \theta_v\}$. This is carried out to each of the l level, Θ_l, partitions with $\{\theta_u, \theta_v\} = \Theta_i - (\Theta_i \cap \Theta_j)$, for all i, $i = j+1$. The slope of the line joining the performance index values for each allocated sensor configuration in this step will differ from station to station. This provides a measure of the inherent sensing difficulty at a station, and the relevance of each sensor to diagnostic performance at that level.

3 An exhaustive list of all alternative distribution schemes is created with the assignment of the $P,(P-1), \ldots,1$ sensors to each of the θ_i parts. The assignments are such that in each instance $\Sigma_{\Theta N} A(\theta_i) = V$, where $A(\theta_i)$ is the sensor number allotment to θ_i and V is the number constraint on the available sensor set for the entire assembly. $A(\theta_i) = 0$ for all θ_i which are not elemental subassemblies.

4 For each assignment in 3 above, J_{b-u} is evaluated as

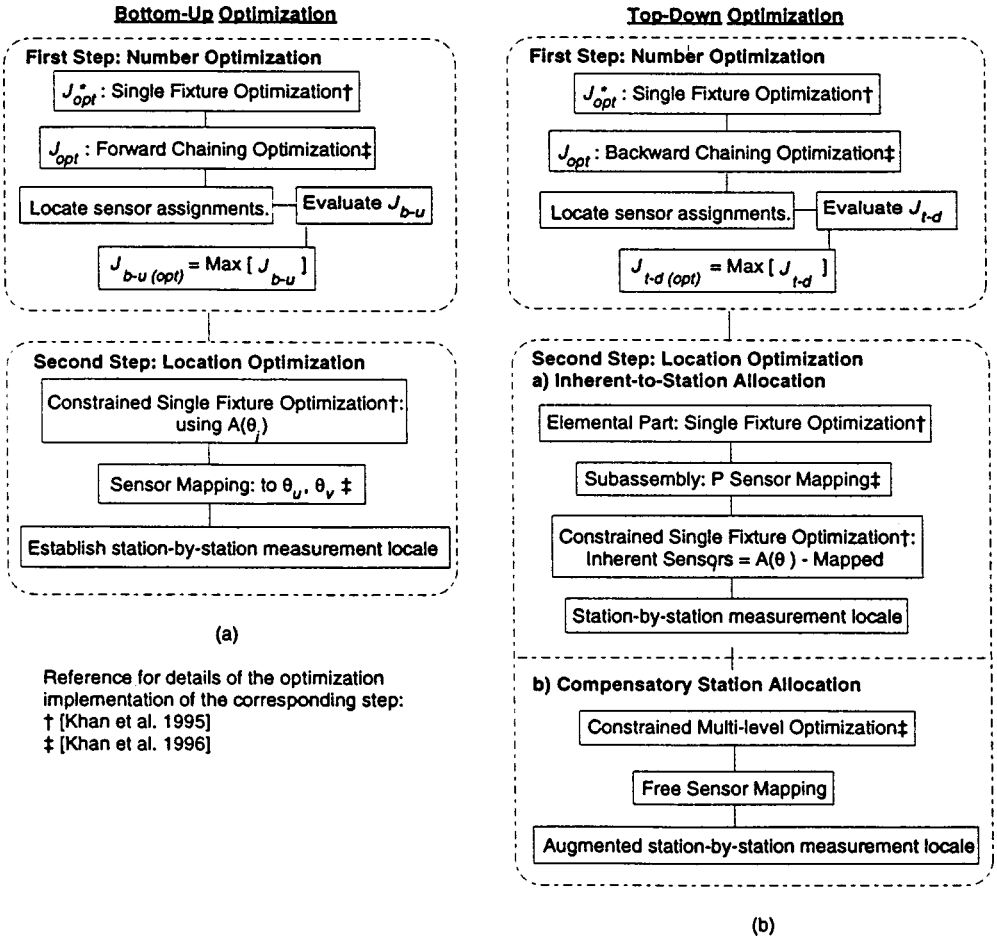

Fig. 4 Optimization implementation sequence: (*a*) bottom-up, (*b*) top-down approaches

$$J_{b-u}=\sum_{l=1,\ldots,N}\ \sum_{i=1,\ldots,\mathrm{card}[\Theta_i]} R_l[\theta_i]J^*_{\mathrm{opt}}(\theta_i)\times\left(\frac{J_{(S_l,A(\theta_i))fwd}}{J_{(S_l,P)fwd}}\right)J_{(S_{|N-1+1|},P)fwd} \tag{3}$$

for all θ_i which are unique elements of Θ; $\theta_i\in\Theta_l \wedge \notin U(\Theta_{l-1})$, and where $U(\Theta_{l-1})$ is the composite set of all partitions to level $l-1$. $J^*_{\mathrm{opt}}(\theta_i)$ corresponds to each fixture's single fixture optima [Eq. (1)], card$[\Theta_l]$ represents the number of parts at level l. $J_{(Si,j)fwd}$ is the diagnostic index resultant from forward chaining optimization with j sensors ($j=P$ or $j=A(\theta_i)$), with optima propagated in the hierarchical model to the station S_i. This is identical to the J_{fwd} computation for end-of-line sensing, but with propagation only to the level of S_i, instead of to the top (measurement station) level [10]. Specifically, for a station S_l, $J_{(S_l,A(\theta_i))fwd}$ is the index value corresponding to an $A(\theta_i)$ sensor distribution from step 3 above, and $J_{(S_l,P)fwd}$ is the index corresponding to a P sensor distribution from step 2. $R_l[\theta_i]$ is a binary decision variable defined as:

$$R_l[\theta_i]=\begin{cases}1 & \text{if } \theta_i\in\Theta_l\\ 0 & \text{if } \begin{cases}\theta_i\neq\Theta_i\\ A(\theta_i)=0\end{cases}\end{cases} \tag{4}$$

The $J^*_{\mathrm{opt}}(\theta_i)$ component of the function computed in step 1 reflects performance with an allocation of sensors dedicated to the part after assembly. The product of this term, with the $J_{(S_{i,j})fwd}$ component, relates part sensing performance to that at station S_i, as this component is the computed performance measure for the composite sub-assembly built up at that station. The $J_{(S|N-i+1|,P)fwd}$ term estimates the (loss of) diagnosability incurred due to sensors being allocated for each level, (l), considered in turn, in lieu of an allocation at each corresponding alternative level, $(N-l+1)$, in the hierarchy. The sensor configuration on each part, and the assembly configuration at the station, together determine J_{b-u} for a particular sensor allocation. Equation (3) may be normalized to simplify computation, using the composite measure of performance effectiveness for all elemental parts, by dividing by:

$$\sum_{\mathrm{card}[\Theta_N]} J^*_{\mathrm{opt}}(\theta) \tag{5}$$

The J_{b-u} estimates are obtained for all the enumerated sensor assignment combinations.

5 The sensor assignment with the highest J_{b-u} value is $J_{b-u(\mathrm{opt})}$, as this corresponds to the sensor number which provides the best fault isolation performance for the Θ_l partitions.

Second Step: Location Optimization

1 For all θ_i with $R_l[\theta_i]=1$, evaluated over $l=1\ldots,N$, single fixture optimization is performed with the $A(\theta_i)$ sensor assignment from the First Step [using Eq. (1)]. The resultant sensor locale is associated with the elements θ_i in the data structure.

2 For every j, where $j=i-1$, a mapping is created of all sensors in the input set $\{\theta_u,\theta_v\}=\Theta_i-(\Theta_i\cap\Theta_j)$, establishing a composite locale for Θ as sensor locale combinations of $\{\theta_u,\theta_v\}$. This creates an optimal map of sensors to corresponding stations at each level.

3 Establish the sensor mapping station-by-station.

The resultant mapping of sensors to stations provides overall optimality, implying optimal fault best-match characteristics and fault discrimination performance.

3.3.2 Optimization: Top-Down Approach. As in the bottom-up approach, the fault set coverage is assumed to be provided by a P sensor distribution for each θ_i. The optimization [Fig. 4(*b*)] proceeds as an iteration through the step sequence in each traversal of the $\langle \mathbf{X}\ \mathbf{T} \rangle$ hierarchy from the top down. (The steps described here are illustrated with an example in Section 4.1.2.)

First Step: Number Optimization

1 Local single fixture optimization is performed, as in step 1 of the bottom-up approach.

2 For each station, backward chaining optimization is used to derive $J_{\text{opt}(bwd)}$ values for $P,(P-1),\ldots,1$ sensor distributions for each consolidated assembled part at that station, $\theta_0=\Theta_j-(\Theta_i\cap\Theta_j)$. In the backward chaining approach, optimization is initiated at the product level. Subsequent optimization is carried out while proceeding downwards in the hierarchy [as in Fig. 3(*b*)] mapping locales from the parent assembly θ_0, at each level.

3 Correspondingly, a list of distribution schemes is created with sensor coverage assignments to each of the θ_i parts. These assignments are also required to satisfy the $\Sigma_{\theta N}A(\theta_i)=V$ condition, as before.

4 For each assignment in 3, a J_{t-d} evaluation is performed, where

$$J_{t-d}=\sum_{l=1,\ldots,N}\ \sum_{i=1,\ldots,\text{card}[\Theta_l]} R_l[\theta_i]J^*_{\text{opt}}(\theta_i) \times\left(\frac{J_{(S_l,A(\theta_i))bwd}}{J_{(S_l,P)bwd}}\right)J_{(S_{|N-l+1|},P)bwd} \tag{6}$$

where $J_{(S_{i,j})bwd}$ is the resultant diagnostic index from a backward chaining optimization routine performed with j sensors, with optima being mapped down the hierarchy to the station S_i. Normalization may be achieved as in the bottom-up case using Eq. (5), with the same effect.

5 The sensor assignment which provides the highest J_{t-d} value is picked as $J_{t-d(\text{opt})}$. The corresponding sensor number provides the overall best-level optimization performance.

Second Step: Location Optimization

(a) Inherent-to-Station Allocation

1 From the sensor assignments of the First Step, the locale corresponding to the smallest l level partition is first decided upon. Local single fixture optimization is used at this partition alone to obtain the optimal positioning/locale for all of the elemental assemblies at this level. These sensor locations are mapped to the lowest level station as the locale of its inherent-to-station allocation component.

2 For the other θ_i assemblies at this level, a P sensor optimization is performed on the composite assembled part. The sensor distribution corresponding to this J_{opt} is mapped onto the component subassemblies at the next level.

3 The difference between the $A(\theta_i)$ sensor allocation and the number of sensors mapped onto the elemental subassembly at the next l level partition is used to obtain the inherent-to-station allocation at this next level. This sensor number serves as the new number constraint. Sensor positions are then determined through a number constrained optimization. These positions are then mapped into the station's coordinates, and constitute the locale of the inherent-to-station allocation at this level.

4 This process is continued on to the highest l level partition.

The sensor set assigned to each station as a consequence of inherent-to-station analysis is now considered ''fixed.'' The difference between the total sensor allocation for each station determined in the First Step and the fixed sensor number are ''free,'' and are allocated in the next, compensatory allocation stage.

(b) Compensatory Station Allocation

5 For each station, the free sensor number is computed and serves as the new sensor number constraint for this next round of optimization.

6 At each level, a free sensor for the elemental subassembly may be assigned locally, or to the station at the level immediately preceding it. A constrained optimization is performed for each of such alternatives enumerated, with diagnostic indices computed for each station configuration. J_{opt}s are computed for each alternative as the sum of the individual values, and the sensor allocation corresponding to the highest J_{opt} value is picked.

7 This sensor allocation is now mapped to the corresponding station to augment the allocation (for local sensing) from step 4.

The process is repeated for each succeeding level, and sensors are successively augmented at each measurement station. The composite of sensors optimized for local performance, and augmented sensors for compensatory coverage of failures at previous levels, provides the overall optimality for the sequence.

3.3.3 Optimization: Special Case Scenarios. This section describes useful modifications to the optimization procedure presented above, to handle the special case scenarios that emerge in certain practical implementations.

One scenario encountered frequently in industrial practice involves dealing with the unavailability of a station or stations for sensor allocation, due to practical considerations of layout, part occlusion, etc. The assumption made in conventional distributed optimization is that sensing allocation in the Second Step is unrestricted to all stations in assembly, and governed only by the optima evaluation. The changed scenario due to station unavailability necessitates a modification in the First Step, to eliminate assignment of sensors to elemental part(s) assembled at the stations(s) identified as unavailable. In addition, to compensate for this (potential) loss in sensing performance, additional subassemblies must be considered for sensor assignment in lieu of these parts. To accommodate this, step 3 of the First Step optimization is modified to incorporate such candidate subassemblies. For a station S_j unavailable for sensing, the choice of subassemblies to be co-opted for assignment instead, along with the other elemental parts, is evaluated automatically as:

$$\bigcup_{\substack{\forall i<j\\ \forall j<k}} S_i\cup[S_k-(S_k\cap S_j)] \tag{7}$$

where S_i, S_j, and S_k are representative of all elements of the partition associated with the corresponding stations. The formulation for the choice of candidate stations presented in Eq. (7) is thus a union of stations above the hierarchy from the station without sensing, with stations below, excepting those common (in the intersection) with the unavailable station in question. The formulation may be extended to accommodate as many unavailable stations as required. Once the additional candidate subassemblies are identified, the optimization proceeds in the normal fashion. An example implementation is provided in the following section.

Another useful provision is the incorporation of a user specification of weights, to preferentially allocate resources by identifying a level of criticality with some specific mis-assemblies. In such situations, weight assignments are typically associated with parts rather than stations. This is in keeping with the notion that ''criticality'' is gauged for a particular part's assembly operation to an extant assembly at the station where the mis-assembly has occured (with some established high probability). Weight assignments are normalized in the First Step, so that for weights w_i associated with θ_i:

$$\sum_{\Theta_N} w_i = 1 \tag{8}$$

The normalized J_{t-d} and J_{b-u} equations (Eqs. 3 and 5, 5 and 6) thus become:

$$J_{t-d} = \sum_{l=1,\ldots,N} \sum_{i=1,\ldots,\mathrm{card}[\Theta_l]} R_l[\theta_i] w_l J^*_{\mathrm{opt}}(\theta_i) \times \left(\frac{J_{(S_l, A(\theta_i))bwd}}{J_{(S_l,P)bwd}} \right) J_{(S_{|N-1+1|},P)bwd}$$

$$J_{b-u} = \sum_{l=1,\ldots,N} \sum_{i=1,\ldots,\mathrm{card}[\Theta_l]} R_l[\theta_i] w_i J^*_{\mathrm{opt}}(\theta_i) \times \left(\frac{J_{(S_l, A(\theta_i))fwd}}{J_{(S_l,P)fwd}} \right) J_{(S_{|N-1+1|},P)fwd} \tag{9}$$

with the denominator in this normalized equation now being unity.

Two forms of analysis can be performed using the optimization procedure involved in the First Step alone without proceeding to the location optimization of the Second Step:

1 A ''what-if'' analysis of the impact of excluding different parts in the assembly sequence from sensing.

2 The effect of ''inserting'' a modular section of assembly with its own optimal sensor assignment in an assembly to be optimized—the modular assembly being independent of (in terms of its sensing configuration) the hierarchy in which it is inserted.

The ''what-if'' analysis is especially pertinent when the available sensor set is too small to guarantee effective coverage of the entire assembly. In such situations, a justifiable proposition may be to concentrate sensing so as to provide comprehensive fault information on a section (of levels) of the assembly hierarchy, rather than to provide information comprehensive to the whole assembly, but inadequate for effective diagnosis at any given level in the assembly. The analysis to decide this is performed for both forms of optimization by evaluating $J_{b-u}(J_{t-d})$ for zero sensor assignments, $A(\theta_i)=0$, for each elemental θ_i in turn. The correspondingly highest value $J_{b-u}(J_{t-d})$ in step 3 would correspond to the sensing locale which provides the best sensor number assignment to some particular section of assembly. The optimization establishes the trade-off criteria by sacrificially omitting sensing for parts which provide the least value of fault discrimination performance for diagnosis. Once this section is isolated, the locale and the station assignments to the rest of the assembly hierarchy may be computed as usual. An example of this analysis is provided in the following section.

A scenario where a consideration of modular subassembly ''insertion'' into an assembly hierarchy is of use is when the modular component has different sensing criteria from the rest of the assembly hierarchy. One example is when a certain module (section) of the assembly sequence has designed slip planes incorporated to compensate for faults in the early stages of assembly. This module may, when considered in isolation, benefit from a top-down approach and may thus be optimized using J_{t-d} criteria. The rest of the assembly may require conventional local sensing, as the need is to localize faults to the smallest part/subassembly immediately at the point of fault occurrence, which can be accomplished using J_{b-u} criteria. This means that the top-down portion of the assembly should be treated as an entity with its own J_{opt}, which, once obtained, is incorporated into the bottom-up optimization for the overall assembly. To accomplish this, the sensor assignment to the station within the module to be inserted is mapped successively downwards in the hierarchy through each sequential antecedent level, until an allocation is available at the level of the elemental parts. The sensing assignment of step 3 may then be performed for the rest of the assembly hierarchy. Local optimization is performed at these levels to obtain a $J_{\mathrm{opt}}(\theta_i)$. These values are used in place of $J^*_{\mathrm{opt}}(\theta_i)$ in Eq. (3) to obtain the overall performance measure.

4 Implementation Scenarios

Both bottom-up and top-down approaches are illustrated here for a standard implementation, using a four layer assembly sequence with four parts. TE locators and initial sensor positions are as shown in Fig. 5. Other configurations are used to explore and illustrate modifications incorporated in the optimization routine to address special case scenarios. For the standard 3-2-1 fixture configuration, effective coverage of the set of enumerated fault conditions is provided by a three sensor distribution for each part. All geometric data used reflect the information available in conventional CATIA-Solid Modeler files. A reconfigurable or flexible sensing layout is required for its implementation in existing assembly lines.

4.1 Standard Implementation. Optimization for a standard distributed sensing configuration is outlined here. Weighting criteria are not utilized, and the assumption is that all assembly stations are candidates for sensing. In both optimization approaches, a complement of ten sensors, $V=10$, is considered to be the available sensor allocation resource.

4.1.1 Optimization: Bottom-Up Approach.

First Step: Number Optimization

Step 1: Local, single fixture optimization is performed for all $\theta_i \in \Theta_N$, based on the formulation of the **d**(**i**) vectors using the TE and candidate sensor positions from CAD data. The resulting optimals are $J^*_{\mathrm{opt}}(\{A\})=1.8515$, $J^*_{\mathrm{opt}}(\{B\})=1.7464$, $J^*_{\mathrm{opt}}(\{C\})=1.0869$, and $J^*_{\mathrm{opt}}(\{D\})=1.9311$. The corresponding sensor lo-

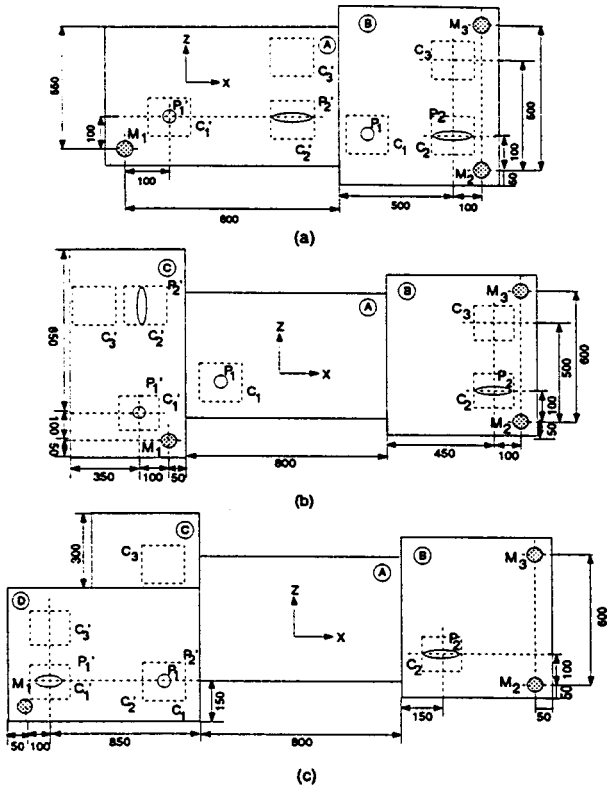

Fig. 5 Assembly part fixturing schematics for (*a*) station S_3, (*b*) station S_2, (*c*) station S_1 (M_1 are candidate sensor locations)

Station	$J_{(S_i,1)fwd}$		$J_{(S_i,2)fwd}$		$J_{(S_i,3)fwd}$	
	Computed	Normalized	Computed	Normalized	Computed	Normalized
S_1	0.1083	0.0608	0.7740	0.4342	1.7822	1.0
S_2	0.0198	0.0129	0.4495	0.2936	1.5312	1.0
S_3	0.0852	0.0453	0.6308	0.3356	1.8798	1.0

(a)

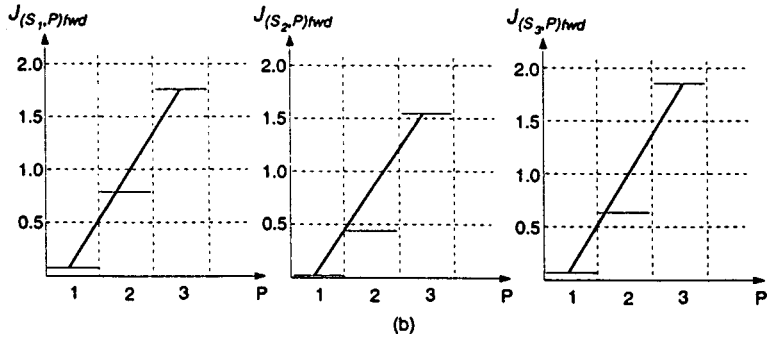

(b)

Fig. 6 Bottom-up approach: (*a*) results of first step optimization, (*b*) graphical representation (linearized) of station sensing performance with 3, 2, and 1 sensors

cale associated with each of these optimized elemental parts provides the best possible local diagnostic performance.

Step 2: Forward Chaining optimization is applied to each station in turn to derive a J_{opt} with 3, 2, 1, sensors. The routine accomplishes this by mapping the best sensor position at each level to the succeeding level, and converging on the optima through an iterative evaluation of the sensor combinations at the new level. For each of the three stations, the computed maximum J_{fwd} and their normalized equivalents are presented in Fig. 6(*a*). Normalization is accomplished by dividing through by the performance index for the best case three sensor configuration, $J_{\text{opt}(fwd)}$, distribution. The resultant values, for use in step 4, are plotted in Fig. 6(*b*).

Step 3: The routine then enumerates all possible sensor allotments to the parts. In the standard optimization approach followed in this section, all parts are assumed to require some sensing allocation. So all ten 3, 2, 1, sensor allotment combinations for the total of $V=10$ available sensing resources are enumerated.

Step 4: J_{b-u} is evaluated as a running summation over the $\langle \mathbf{X}\ \mathbf{T} \rangle$ traversal for $R_3[\{A\}]=1$, $R_3[\{B\}]=1$, $R_2[\{C\}]=1$, and $R_1[\{D\}]=1$, with all other $R_l[(\theta_i)]$ being 0. For example, among the sensor distributions enumerated in step 3, the optimal of (3, 3, 1, 3) for the $\{\{A\}\{B\}\{C\}\{D\}\}$ set, J_{b-u}, is evaluated as:

$$J_{b-u}=(J^*_{\text{opt}}(A)\times J_{(S_1,3)fwd})+(J^*_{\text{opt}}(B)\times J_{(S_1,3)fwd}) + (J^*_{\text{opt}}(C)\times J_{(S_2,1)fwd})+(J^*_{\text{opt}}(D)\times J_{(S_1,3)fwd}) \quad (10)$$

Step 5: The highest J_{b-u} value, corresponding to (3, 3, 1, 3), provides a $J_{b-u(\text{opt})}$ of 0.8378.

Second Step: Location Optimization

Step 1: Given the $R_l[\theta_i]$ values of step 4 in the First Step and the optimal (3, 3, 1, 3) sensor assignment, single fixture optimization is performed for each elemental part using the sensor assignments as the number constraint for the optimization. The resultant sensor assignments associated with the parts in the data structure are provided in Fig. 7. The data structure associates the parts with their respective initial assembly stations.

Step 2: The mapping procedure then creates the sensing allocation to the corresponding station, establishing a composite locale for each of the parts.

Step 3: The mapping procedure is repeated for each station (Fig. 8).

4.1.2 Optimization: Top-Down Approach.

First Step: Number Optimization

Step 1: Optimals are obtained using local single fixture optimization as in step 1 of the bottom-up approach.

Step 2: Backward chaining optimization is applied to each station to derive a J_{opt} with 3, 2, 1 sensors. For each transition, the parent assembly θ_o sensor locale is mapped downwards to the antecedent level to determine allocation and performance at that level. For each of the three stations, the computed maximum J_{bwd} and their normalized equivalents are presented in Fig. 9(*a*). Normalization is accomplished by dividing through by the best case three sensor distribution, $J_{(S_1,3)bwd}$. The resultant values, for use in Step 4, are plotted in Fig. 9(*b*).

Part - Sensor Allotment		S_{1x}	S_{1z}	S_{2x}	S_{2z}	S_{3x}	S_{3z}
A	3	–	–	–	–	79.42	151.26
		–	–	–	–	856.24	203.23
		–	–	–	–	712.03	385.37
B	3	–	–	–	–	957.90	149.91
		–	–	–	–	1406.65	150.08
		–	–	–	–	1267.64	278.19
C	1	–	–	347.16	751.53	–	–
		–	–	–	–	–	–
		–	–	–	–	–	–
D	3	135.83	146.98	–	–	–	–
		928.75	156.71	–	–	–	–
		206.33	295.95	–	–	–	–

Note: All dimensions in respective assembly station coordinates

Fig. 7 Bottom-up approach: results of second step optimization

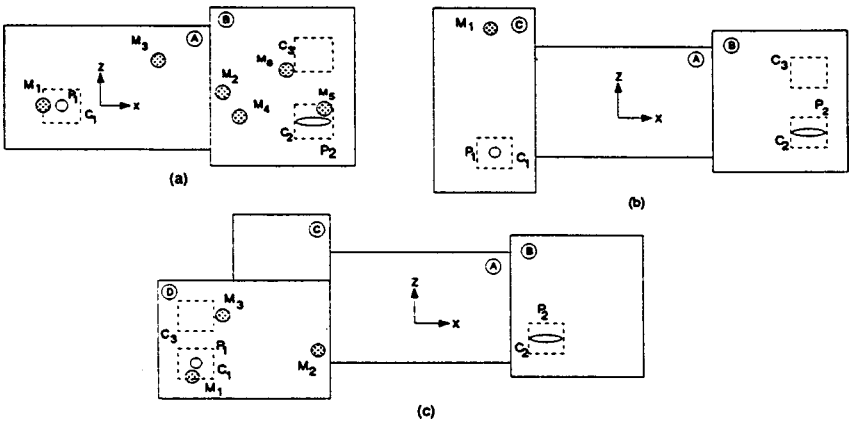

Fig. 8 Bottom-up approach—overall sensing distribution: (*a*) station S_3, (*b*) station S_2, and (*c*) station S_1

Step 3: Under the assumption that all parts require sensing allocation, the $V=10$ sensing resources are allotted, in combinations of 3, 2, and 1 each, to the parts. An exhaustive listing of all such possible allotments is created.
Step 4: For this $\langle \mathbf{X}\ \mathbf{T}\rangle$ traversal, $R_l[\theta_i]$ and the optimal sensor assignments of (3, 3, 1, 3) for the $\{\{A\}\{B\}\{C\}\{D\}\}$ set are identical to those in the enumeration for the bottom-up approach. This is merely coincidental however, as the formulations for each approach are distinct. As a result of this similarity, the J_{t-d} formulation mirrors that for the corresponding bottom-up approach:

$$J_{t-d}=(J^*_{\text{opt}}(A)\times J_{(S_1,3)bwd})+(J^*_{\text{opt}}(B)\times J_{(S_1,3)bwd}) + (J^*_{\text{opt}}(C)\times J_{(S_2,1)bwd})+(J^*_{\text{opt}}(D)\times J_{(S_3,3)bwd}) \quad (11)$$

Step 5: The optimal (3, 3, 1, 3) allocation provides a $J_{t-d(\text{opt})}$ value of 0.8365.

Second Step: Location Optimization

(a) Inherent-to-Station Allocation

Step 1: As $R_1[D]=1$, local single fixture optimization may be directly used at this first level partition to obtain the optimal sensor positioning. These coordinates, being mapped directly to station 1, are thus identical to those obtained in the bottom-up approach.
Step 2: The three sensor optimization is performed for the other component in this partition, $\{\{ABC\}\}$. The sensor distribution is now mapped to component subassemblies $\{AB\}$ and $\{C\}$, using part boundaries in the CAD Body Coordinate frame as dimensional extents.
Step 3: As element $\{C\}$ is provided with a single sensor allocation from the First Step, the single mapped location from step 2 is consequently also its sensor allocation.
Step 4: Component $\{AB\}$ in the next level partition is now optimized with a three sensor constraint, and mapping continued to the level of $\{\{A\}\{B\}\}$. The resultant mapping is a single sensor to $\{A\}$ and two sensors to $\{B\}$.

The resultant inherent-to-station allocation is shown in Fig. 10.

(b) Compensatory Station Allocation

Step 5: The free sensor number (Fig. 11) is thus three. The number constraints are (2, 1) for $\{\{A\}\{B\}\}$.
Step 6: As both free sensor elements are at the same $l=4$ level, we start with that for the larger free sensor allotment at this level (with two sensors), $\{\{A\}\}$. J_{opt} is computed using a constrained optimization on the two sensor positions for stations S_2 and S_3.

Station	$J_{(S_1,1)bwd}$		$J_{(S_1,2)bwd}$		$J_{(S_1,3)bwd}$	
	Computed	Normalized	Computed	Normalized	Computed	Normalized
S_1	0.0025	0.0019	0.5252	0.2785	1.8858	1.0
S_2	0.0091	0.0048	0.9864	0.5190	1.9005	1.0
S_3	0.0714	0.0360	0.9996	0.5046	1.9809	1.0

(a)

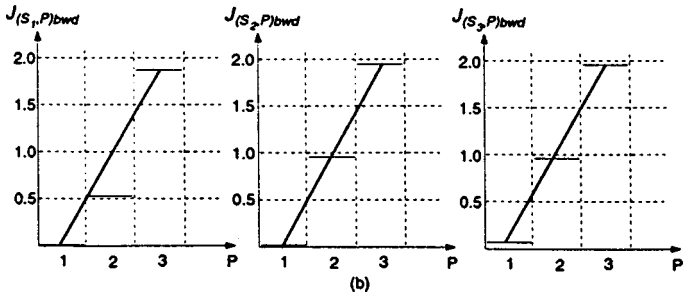

Fig. 9 Top-down approach: (*a*) results of the first step optimization, (*b*) graphical representation (linearized) of station sensing performance with 3, 2, and 1 sensors

The optimization analysis inherits previously allocated sensors, and thus accounts for performance due to previous sensor assignments made in the Inherent-to-Station allocation step above. The evaluations for the resultant combination are shown in Fig. 11(*a*).
Step 7: The highest J_{opt} value of 2.902 is picked, with the corresponding two sensor enhancement to station S_2.
Step 8: The process is repeated to determine the single free sensor allocation corresponding to $\{\{B\}\}$. Optimization is carried out on the two alternatives with a single sensor enhancement to the sensor distribution from the Inherent-to-Station sensing of a). The results are shown in Fig. 11(*b*). The highest J_{opt} of 3.0587 is picked with its corresponding sensor enhancements: the enhancements being made to station S_2 (Fig. 11(*c*)).

Sensor allocation for all stations as a consequence of the top-down approach analysis is captured in Fig. 12.

A diagnostic performance comparison may be made with equivalent end-of-line sensing based fault diagnosability at a level of assembly. The $J_{b-u(\text{opt})}$ and $J_{t-d(\text{opt})}$ values of 0.8378 and 0.8365 are average measures of performance in the distributed sensing case, at an intermediate level of assembly. Equivalent end-of-line optimum diagnosability in the four-layer sequence,

Part - Sensor Allotment		S_{1x}	S_{1z}	S_{2x}	S_{2z}	S_{3x}	S_{3z}	Allocated	Free
A	3	–	–	–	–	107.41	187.26	1	2
		–	–	–	–	–	–		
		–	–	–	–	–	–		
B	3	–	–	–	–	1313.82	137.38	2	1
		–	–	–	–	1153.30	410.21		
		–	–	–	–	–	–		
C	1	–	–	233.08	167.02	–	–	1	0
		–	–	–	–	–	–		
		–	–	–	–	–	–		
D	3	135.83	146.98	–	–	–	–	3	0
		928.75	156.71	–	–	–	–		
		206.33	295.95	–	–	–	–		

Note: All dimensions in respective assembly station coordinates

Fig. 10 Top-down approach—second step optimization: Inherent-to-station allocation results

Station - Sensor Distribution		Diagnosability Index		
		$J_{opt}(S_2)$	$J_{opt}(S_3)$	J_{opt}
2	0	0.9889	1.9131	2.9020
1	1	0.9525	1.9223	2.8748
0	2	0.0406	1.9253	1.9659

(a)

Station - Sensor Distribution		Diagnosability Index		
		$J_{opt}(S_2)$	$J_{opt}(S_3)$	J_{opt}
1	0	1.1458	1.9131	3.0587
0	1	0.9889	1.9223	2.9112

(b)

Part - Sensor Allotment		S_{1x}	S_{1z}	S_{2x}	S_{2z}	S_{3x}	S_{3z}
A	2	–	–	599.14	201.32	–	–
		–	–	1797.60	657.91	–	–
		–	–	–	–	–	–
B	1	–	–	1575.56	337.45	–	–
		–	–	–	–	–	–
		–	–	–	–	–	–

Note: All dimensions in respective assembly station coordinates

(c)

Fig. 11 Top-down approach—second step optimization: (*a*) combinations for part A allotment computation, (*b*) combinations for part B allotment computation, and (*c*) compensatory station allocation results

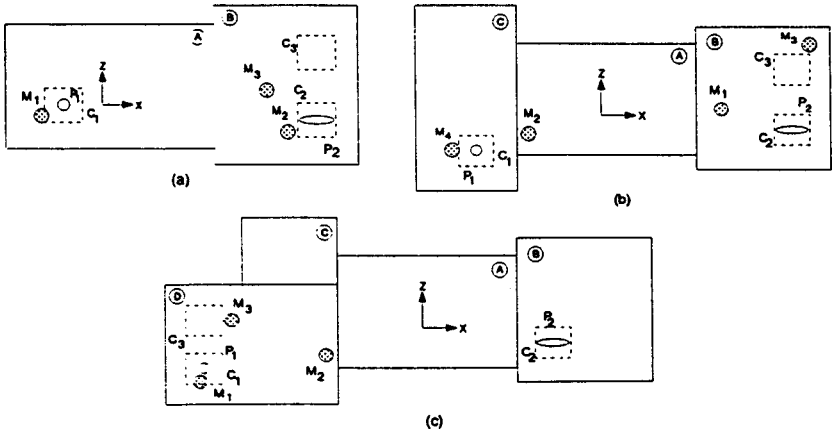

Fig. 12 Top-down approach—overall sensing distribution (*a*) station S_3, (*b*) station S_2, and (*c*) station S_1

computed at this intermediate *AB* level are 0.7748 and 0.6137. Percentage performance enhancements due to distributed sensing are thus 8% and 36% in each instance.

4.2 Special Case Scenarios

4.2.1 Station Unavailability. The implication of the station unavailability scenario necessitates a modification of step 3 of the First Step Optimization (as noted in Section 3.3.3), to accommodate the elimination of the elemental part(s) at the station(s) in question and the incorporation of a non-elemental subassembly for sensor allocation in its place. To illustrate, the standard three level, four part, subassembly is considered, but with station S_2 assumed unavailable. Consequently, a sensor assignment to C, $(R_2[\{C\}]=1)$, is no longer feasible. In this in-

stance, Eq. (7) provides the set of assignable subassemblies for sensing:

$$S_1 \cup [S_3 - (S_3 \cap S_2)] = \{\{A\}\{B\}\{ABC\}\{D\}\} \tag{12}$$

Once the subassemblies are identified for allotment, Eqs. (3) and (6) are modified correspondingly. For example, the equations that correspond to one of the enumerated combinations (3, 3, 2, 1) are:

$$J_{b-u} = (J^*_{\text{opt}}(A) \times J_{(S_1,3)fwd}) + (J^*_{\text{opt}}(B) \times J_{(S_1,3)fwd}) + \frac{(J_{(S_1,2)fwd} \times J_{(S_3,3)fwd}) + \left[J^*_{\text{opt}}(D) \times \frac{J_{(S_1,1)fwd}}{J_{(S_1,3)fwd}} \right] J_{(S_3,3)fwd}}{4} \tag{13}$$

$$J_{t-d} = (J^*_{\text{opt}}(A) \times J_{(S_1,3)bwd}) + (J^*_{\text{opt}}(B) \times J_{(S_1,3)bwd}) + \frac{(J_{(S_1,2)bwd} \times J_{(S_3,3)bwd}) + \left[J^*_{\text{opt}}(D) \times \frac{J_{(S_1,1)bwd}}{J_{(S_1,3)bwd}} \right] J_{(S_3,3)fwd}}{4} \tag{14}$$

The second step allocation now proceeds exactly as in the standard implementation.

4.2.2 First Step Analysis: Part Exclusion. A scenario similar to station unavailability corresponds to another practical consideration: determining which part may be excluded from sensing when sensing resources are low. The requirement is that resources be maximally beneficial and only allocated to parts whose fault discrimination performance is maximally enhanced.

Consider, for example, a total sensor allocation resource V of eight sensors. A conventional analysis aimed at comprehensive sensing for the entire assembly provides for a (2, 2, 2, 2) assignment to $\{\{A\}\{B\}\{C\}\{D\}\}$. The corresponding index values computed for Bottom-up and Top-down optimizations are:

$$J_{b-u(\text{opt})} = 0.3823 \tag{15}$$

$$J_{t-d(\text{opt})} = 0.3840 \tag{16}$$

The ''what-if'' analysis utilizes the First Step optimization to explore the effect of sacrificially omitting sensing allocated to each part, in turn. To accomplish this, a modification in step 3 of the Bottom-up and Top-down approaches is made to allow for a zero sensor assignment to $\{A\}$, $\{B\}$, $\{C\}$, and $\{D\}$, in turn. The twelve resultant allotments are then evaluated using Eqs. (3) and (6) in step 4. The resultant index value in the Bottom-up approach corresponding to a (3, 2, 0, 3) assignment (no part C sensing allotment) is:

$$J'_{b-u(\text{opt})} = 0.6041 \tag{17}$$

and the value for the Top-down approach corresponding to a (3, 3, 0, 2) assignment (no part C sensing) is:

$$J'_{t-d(\text{opt})} = 0.6411 \tag{18}$$

The comparison with the standard optimization approach's index values in Eqs. (15) and (16) reveals a 45.8 percent and a 44.4 percent improvement in overall optimality for Bottom-up and Top-down approaches respectively, with this sacrificial, preferential allotment procedure incorporated in the optimization.

5 Summary and Conclusion

The effectiveness of system-level fault diagnosis in complex systems, such as multi-fixture sheet-metal assembly, is critically dependent on the effectiveness of the sensor layout, i.e., in identifying, localizing, and isolating faults. As complexity increases with an increase in the number of assembly parts, levels of assembly, etc., the fault discrimination capability of the single measurement station of traditional end-of-line sensing is overwhelmed by the proliferation of possible faults. A distributed sensing approach has been presented here to address this.

The approach utilizes a two-step hierarchical optimization procedure. Two practical requirement-driven choices for optimization have been presented, depending on if immediate detection is required (Bottom-Up approach) or if faults are to be revisited (Top-Down approach). The procedure involves decomposition and sequential quadratic programming optimization. Formulated part-specific and process-specific constraints were applied at each decomposed level, with optimization proceeding as a state and design variable transition function evaluation in each traversal of the directed graph. The tree of optimal sequences was coordinated for each traversal in the location optimization step to converge on the overall optimal distribution. The optimization technique used was found to be efficient and robust to initial value choice. However, any alternative technique may be substituted for use within the proposed framework to improve performance. The focus and novelty of the approach lies not in the specific optimization technique choice, but in the use of the proposed hierarchical methodology to achieve the optimal sensor distribution.

References

[1] Ceglarek, D., Shi, J., and Wu, S. M., 1994, ''A Knowledge-based Diagnosis Approach For The Launch Of The Auto-body Assembly Process,'' ASME J. Eng. Ind., **116**, No. 4, pp. 491–499.

[2] de Kleer, J., and Williams, B. C., 1987, ''Diagnosing Multiple Faults,'' Artif. Intel., **32**, pp. 97–130.

[3] Reiter, R., 1987, ''A Theory Of Diagnosis From First Principles,'' Artif. Intel., **32**, pp. 57–96.

[4] Wu, T. D., 1991, ''Problem Decomposition Method For Efficient Diagnosis And Interpretation Of Multiple Disorders,'' Comput. Methods Programs Biomed., **35**, No. 4, pp. 239–250.

[5] Ceglarek, D., and Shi, J., 1996, ''Fixture Failure Diagnosis For Autobody Assembly Using Pattern Recognition,'' ASME J. Manuf. Sci. Eng., **118**, No. 1, pp. 55–66.

[6] Genesereth, M. R., 1984, ''The Use Of Design Descriptions In Automated Diagnosis,'' Artif. Intel., **24**, pp. 411–436.

[7] Khan, A. M., Ceglarek, D., Shi, J., Ni, J., and Woo, T. C., 1999, ''Sensor Optimization For Fault Diagnosis In Single Fixture Systems: A Methodology,'' ASME J. Manuf. Sci. Eng., **121**, No. 1, pp. 109–117.

[8] De Fazio, T. L., and Whitney, D. E., 1987, ''Simplified Generation Of All Mechanical Assembly Sequences,'' IEEE J. Robotics Automation, **3**, pp. 640–705; and 1998, Corrections, IEEE J. Robotics Automation, **4**, pp. 705–708.

[9] Homem de Mello, L. S., and Sanderson, A. C., 1991, ''Representation Of Mechanical Assembly Sequences,'' IEEE Trans. Robotics Automation, **7**, pp. 211–227.

[10] Khan, A. M., Ceglarek, D., and Ni, J., 1998, ''Sensor Location Optimization For Fault Diagnosis in Multi-Fixture Assembly Systems,'' ASME J. Manuf. Sci. Eng., **120**, No. 4, pp. 781–792.

[11] Zeigler, B. P., 1992, ''Systems Formulation of a Theory of Diagnosis from First Principles,'' IEEE Trans. Reliab., **41**, No. 1.

[12] Ceglarek, D., and Shi, J., 1998, ''Design Evaluation of Sheet Metal Joints for Dimensional Integrity,'' ASME J. Manuf. Sci. Eng. **120**, No. 2, 452–460.

[13] *Matlab: Optimization Toolbox User's Guide*, The MathWorks, Inc.